Regular paper

Miniaturized Circularly Polarized Patch Antenna Using Coupled Shorting Strip and Capacitive Probe Feed

Hongyu Shi, Junwei Shi, Jianxing Li, Juan Chen, Zhiyuan Li, Shitao Zhu, Tayyab Ali Khan, Anxue Zhang

PII: S1434-8411(18)31906-X
DOI: https://doi.org/10.1016/j.aeue.2018.11.022
Reference: AEUE 52588

To appear in: *International Journal of Electronics and Communications*

Received Date: 7 August 2018
Revised Date: 28 October 2018
Accepted Date: 10 November 2018

Miniaturized Circularly Polarized Patch Antenna Using Coupled Shorting Strip and Capacitive Probe Feed

Dr. Hongyu, Shi (Associate Professor)
School of Electronic and Information Engineering, Xi'an Jiaotong University, Xi'an, China
Email: hongyushi@xjtu.edu.cn

Dr. Jianxing, Li (Corresponding author)
School of Electronic and Information Engineering, Xi'an Jiaotong University, Xi'an, China
Email: jianxingli.china@xjtu.edu.cn

Miss Junwei, Shi (Master Student)
School of Electronic and Information Engineering, Xi'an Jiaotong University, Xi'an, China
Email: sjw777@stu.xjtu.edu.cn

Dr. Juan, Chen (Professor)
Shenzhen Research School, Xi'an Jiaotong University, Shenzhen, China
Email: chen.juan.0201@mail.xjtu.edu.cn

Mr. Zhiyuan, Li (Master Student)
School of Electronic and Information Engineering, Xi'an Jiaotong University, Xi'an, China
Email: lizhiyuan@stu.xjtu.edu.cn

Dr. Shitao, Zhu
School of Electronic and Information Engineering, Xi'an Jiaotong University, Xi'an, China
Email: shitaozhu@xjtu.edu.cn

Mr. Tayyab Ali, Khan (Master Student)
School of Electronic and Information Engineering, Xi'an Jiaotong University, Xi'an, China
Email: tayyabali114@yahoo.com

Dr. Anxue, Zhang (Professor)
School of Electronic and Information Engineering, Xi'an Jiaotong University, Xi'an, China
Email: anxuezhang@mail.xjtu.edu.cn

Miniaturized Circularly Polarized Patch Antenna Using Coupled Shorting Strip and Capacitive Probe Feed

Hongyu Shi[1], Junwei Shi[1], Jianxing Li[1,*], Juan Chen[2], Zhiyuan Li[1], Shitao Zhu[1], T. A. Khan[1], and Anxue Zhang[1]

[1]School of Electronic and Information Engineering, Xi'an Jiaotong University, Xi'an, China

[2]Shenzhen Research School, Xi'an Jiaotong University, Shenzhen, China

Email: jianxingli.china@xjtu.edu.cn ([*]corresponding author)

ABSTRACT

This paper proposes a single-feed miniaturized circularly polarized (CP) patch antenna aimed to cover Chinese BeiDou navigation satellite system (BDS) B3 band (1268.52±10.23 MHz). Four unbalanced circular patches as perturbation elements are loaded onto corners of a square patch radiator to ensure CP property. To simultaneously realize miniature size and adequate CP bandwidth, each circular patch is coupled to an L-shaped shorting strip consisting of a horizontal arc-shaped strip connected to the ground plane through a vertical shorting pin. In addition, a capacitive probe feed fulfilled by embedding an annular gap is used to compensate large probe inductance due to thick substrate, and therefore good impedance matching can be obtained. The antenna occupies an overall size of $\lambda_0/8 \times \lambda_0/8 \times \lambda_0/13.6$, where λ_0 denotes the free space wavelength at 1268 MHz. Experimental results show that it achieves a 10-dB return loss impedance bandwidth of 75 MHz (1237 MHz – 1312 MHz) and a 3-dB axial ratio (AR) bandwidth of 31 MHz (1253 MHz – 1284 MHz). The measured 3-dB AR beamwidth and CP gain are above 170° and 4.0 dBic, respectively, across the entire BDS B3 band.

Key words: BeiDou navigation satellite system (BDS); coupled shorting strip; capacitive probe feed; circular polarization (CP); miniaturized patch antenna.

1. INTRODUCTION

Antennas are essential components for wireless communication systems. In the past several decades, much research efforts have been devoted to novel antenna designs to satisfy more and more challenging requirements [1–7]. It is well known that circularly polarized (CP) patch antennas have been extensively applied to global navigation satellite systems (GNSS), because CP waves have capabilities to combat Faraday rotation and improve signal reception robustness [8–11]. However, GNSS receivers exhibit severe vulnerability to jammers as a result of the relatively weak signal strength received on the earth [12]. Adaptive anti-jam GNSS arrays are commonly deployed in military scenarios to overcome this issue [13–15]. Due to the rigorous space constraints for platforms involving small unmanned aerial vehicles and precision-guided missiles, realizing miniature antenna elements becomes a prerequisite in implementing such an adaptive array.

Many techniques can be found from the literature on investigating miniaturized patch antenna designs, such as utilizing high dielectric substrates [16–18], inserting slots [19] and slits [20], [21] on the patch radiator, employing metamaterials [21–26], loading lumped elements [27], and introducing shorting pins [28–32]. Amongst them, it may be the most straightforward mean to reduce patch sizes with the use of high dielectric substrates. In [16–18], high dielectric ceramic substrates were utilized and miniaturized patch sizes of below $\lambda_0/9 \times \lambda_0/9$ were obtained. This technique, however, exhibits disadvantages associated with narrow bandwidth, challenging fabrication and impedance matching process, and expensive cost. In comparison, other ways of inserting slots and slits and employing metamaterials are relatively ease of implementation and inexpensive but less effective in size miniaturization. Those antennas depending on these techniques typically occupy aperture sizes of above $\lambda_0/4 \times \lambda_0/4$ [20–22]. In [27], four lumped capacitors and twenty inductive pins have been loaded onto a dual-band coupled double loop GPS antenna, resulting in a rather compact size of $\lambda_0/8 \times \lambda_0/8 \times \lambda_0/19.4$. However, it requires laboursome soldering and particular quadrature feed network. Besides, additional ohmic loss may be induced due to the parasitic resistance of capacitors.

Placing metallic shorting pins between the patch radiator and ground plane is acknowledged as the most distinguished technique in developing size-reduced patch antennas [28]. Recently, shorting strips coupled rather than directly connected to the patch radiator, usually denoted as coupled shorting strips, have drawn much research attention [29–32]. In [29], the patch size of a linearly polarized antenna was diminished by 74% to be approximate $\lambda_0/11.4 \times \lambda_0/11.2$. A size reduction as large as 82% has been obtained in the CP patch antenna [30]. However, its relatively narrow CP bandwidth prevents it from GNSS applications. In [31], the mechanism of bandwidth enhancement underlying coupled shorting strips was analyzed, and a compact dual-feed CP patch antenna with a total size of $\lambda_0/7 \times \lambda_0/7 \times \lambda_0/15$ was subsequently designed. To ease the feed network complexity, a single-feed cross-aperture coupled CP patch antenna was investigated owing a patch size of $\lambda_0/5.5 \times \lambda_0/5.7$ [32]. This antenna, nevertheless, suffers from relatively high back radiation.

In this paper, a single-feed miniaturized CP patch antenna is proposed for Chinese BeiDou navigation satellite system (BDS) applications. It operates at the BDS B3 band and possesses an overall size of $\lambda_0/8 \times \lambda_0/8 \times \lambda_0/13.6$. Four L-shaped coupled shorting strips are employed to reduce the patch size but retain adequate CP bandwidth. The antenna is fed using a capacitive probe feed to negate the large probe inductance because of the thick air substrate.

The CP and impedance matching performance of the antenna can therefore be independently tuned. This can significantly save optimization time consumption. The antenna has been simulated using Ansoft HFSS 14.0 and demonstrated by experiments.

2. ANTENNA DESIGN AND ANALYSIS

2.1. Geometrical configuration

Fig. 1 shows the geometrical configuration of the proposed single-feed miniaturized CP patch antenna. The antenna comprises an $L_p \times L_p$ square patch radiator printed on an $L_s \times L_s$ Taconic RF-60 substrate (ε_r = 6.15, tanδ = 0.0028, and thickness H_1 = 3.18 mm). Loaded onto corners of the patch radiator are four unbalanced circular patches possessing radii of R_1, R_2, R_3, and R_4, respectively. These circular patches function as necessary perturbation elements to excite two orthogonal degenerate modes, and consequently realize CP radiation [33]. Four L-shaped coupled shorting strips are introduced along the two diagonals to reduce the antenna size, and each of them consists of a horizontal arc-shaped strip coupled to the individual circular patch and a vertical shorting pin connected to the ground plane. The strip width and gap from the circular patch are denoted as W_s and g_1, respectively. All arc-shaped strips are subtended by an angle of 90°. The shorting pins with an identical radius of R_p are positioned at ($\pm s$, $\pm s$), as depicted in Fig. 1(a). The radius of the probe feed is selected as 0.35 mm in the proposed antenna design.

In theory, the achievable bandwidth of a patch antenna is expected to decrease as a result of size reduction [34]. Hence, an H_2 thick air gap is sandwiched between the top substrate and ground plane to enhance bandwidth. In addition, the coupled shorting strips can be equivalent to series LC loading. On one hand, increasing inductance L or capacitance C leads to a more compact antenna size. On the other hand, decreasing inductance L or increasing capacitance C may improve potential bandwidth due to the lowered quality factor. Thus, the employment of coupled shorting strips efficiently offers an additional freedom that can benefit bandwidth enhancement.

Though thicker substrates can promise wider realizable CP bandwidth, acceptable impedance matching is frequently unattainable owing to the large probe inductance for thicker substrates [35]. Resultantly, an annular gap capacitor is embedded in series with the probe inductance. The radius and width of the annular gap are denoted as R_5 and g_2, respectively. It should be noted that the series capacitor not only compensates the probe inductance but also allows an antenna design featuring that CP and impedance matching performance can be independently tuned, which avoids time-consuming and complex optimization.

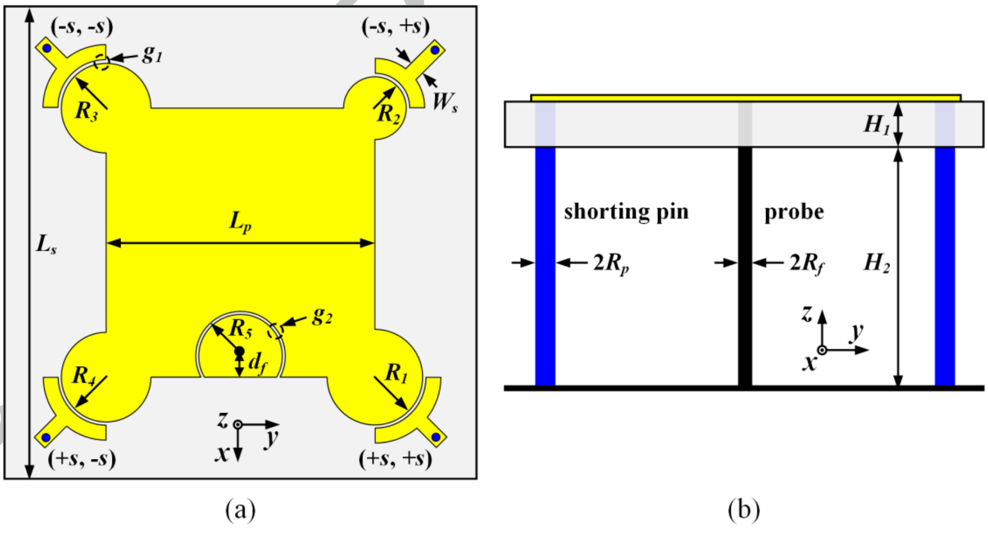

Fig. 1. Geometrical configuration of the proposed miniaturized CP patch antenna.

(a) Top view. (b) Side view.

After several design iterations, the final structural parameters of the antenna have converged to those summarized in Table 1. The antenna occupies an overall size of 30 mm × 30 mm × 17.3 mm, demonstrating a compact electrical size of $\lambda_0/8 \times \lambda_0/8 \times \lambda_0/13.6$ with respect to the free space wavelength at the center frequency of BDS B3 band, i.e. 1268.52 MHz.

Table 1. Structural parameters of the proposed miniaturized CP patch antenna.

Parameter	H_1	H_2	L_s	L_p	R_1	R_2	R_3	R_4
Value (mm)	3.18	14.1	30.0	18.0	3.2	2.1	3.0	3.0
Parameter	R_5	R_p	W_s	s	g_1	g_2	d_f	R_f
Value (mm)	2.8	0.5	1.0	13.0	0.2	0.2	1.4	0.35

2.2. Parametric studies

Parametric studies are carried out by simulations to study the effects of coupled gap width g_1 and annular gap capacitor width g_2 on the return loss and broadside axial ratio (AR) response of the proposed antenna. We should note that each time only one parameter is varied and all other parameters are maintained the same as those listed in Table 1.

Fig. 2 presents the simulated return loss and broadside AR performance when changing the coupled gap width g_1. It shows clearly that decreasing g_1 can efficiently reducing the resonant frequency of the proposed antenna. In another word, the electrical size of the antenna shrinks accordingly. The antenna resonates beyond 1.5 GHz in the absence of the coupled gap. When g_1 is narrowed from 0.6 mm to 0.2 mm, the resonant frequency shifts from 1.4 GHz to 1.26 GHz. Besides, we can further find that the minimum achievable broadside AR is deteriorated once g_1 deviates from 0.2 mm.

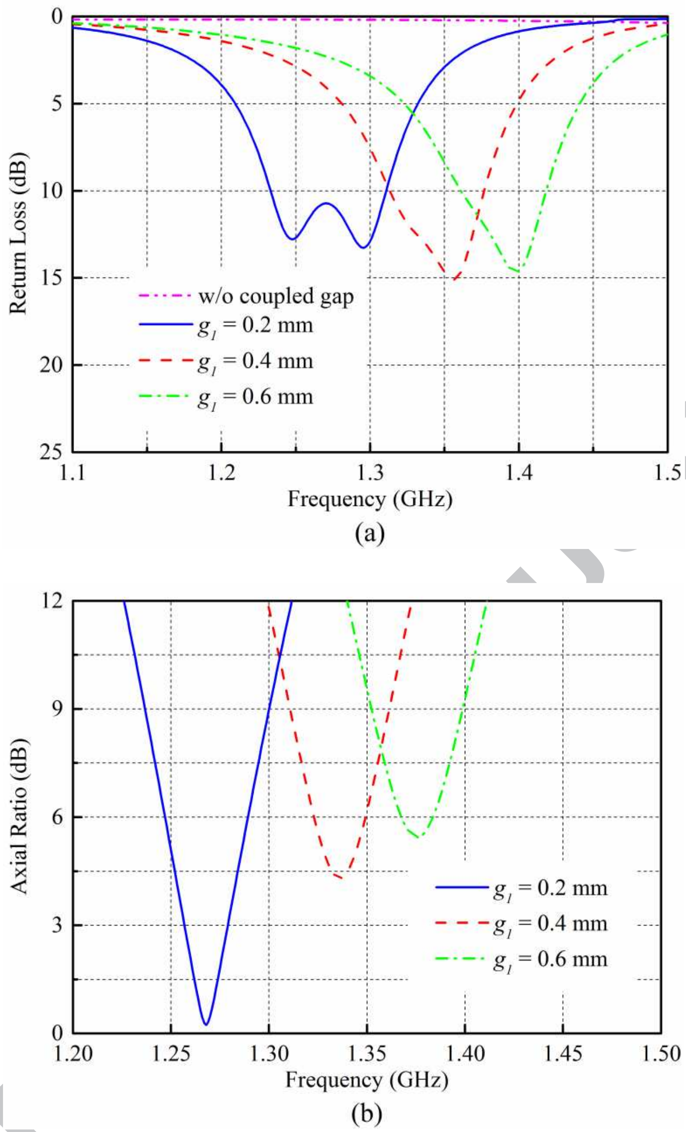

Fig. 2. Simulated return loss and broadside AR for different coupled gap width.

The simulated return loss and broadside AR when varying the annular gap capacitor width g_2 are plotted in Fig. 3. It can be apparently observed that g_2 is fairly effective to tune impedance matching of the proposed antenna. Meanwhile, the broadside AR performance almost keeps unchanged. In detail, the return loss of the antenna is pretty poor in the absence of the annular gap. When g_2 decreases from 0.6 mm to 0.2 mm, the resultant capacitance is increased, which becomes sufficiently large to compensate the reactance induced by the long probe feed. This enables an independent freedom to obtain good impedance matching.

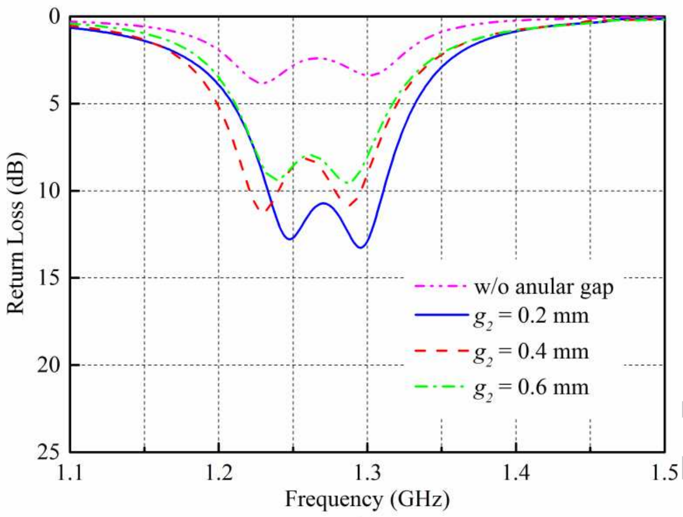

(a)

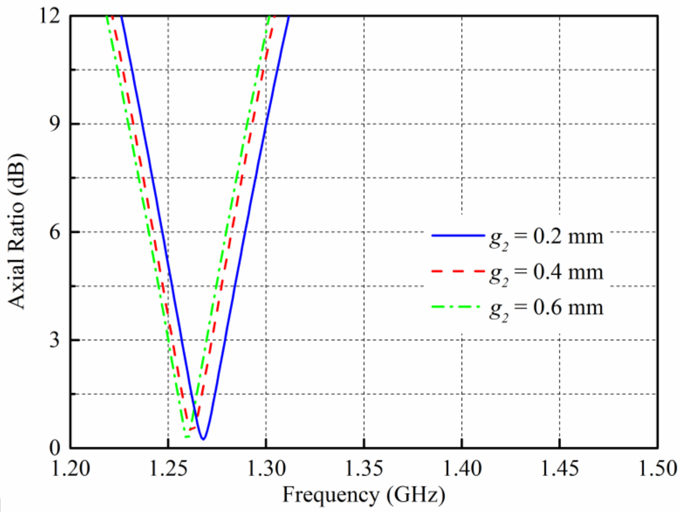

(b)

Fig. 3. Simulated return loss and broadside AR for different annular gap width.

To conclude, a concise design procedure for the proposed antenna can be derived as follows: 1) select appropriate patch length (L_p) and coupled shorting strips (R_p and g_1) according to the required frequency band; 2) choose the radii of corner-loaded circular patches (R_1, R_2, R_3, and R_4) to generate excellent CP characteristic; 3) tune the annular gap width (g_2) to achieve good impedance matching.

3. EXPERIMENTAL RESULTS

A prototype of the proposed antenna has been manufactured and assembled. The photograph of the antenna prototype is depicted as an inset in Fig. 4. Two metal screws are used to fasten an SMA connector underneath the ground plane so as to feed the antenna. An Agilent E8363B vector network analyzer is employed to measure the antenna performance. Fig. 4 presents the simulated and measured return loss, showing that the measured 10-dB return loss impedance bandwidth is ranging from 1237 MHz to 1312 MHz (75 MHz). Discrepancies between the measured and simulated results are probably owing to the additional insertion loss induced by the inclusion of the SMA connector. Besides, the loss tangent of the substrate may be larger than the nominal value. The ground plane, patch radiator as well as probe feed and shorting pins are assigned as PEC boundaries in the simulations, whereas all of them are made from lossy metals in the prototype. The simulated and measured broadside AR are illustrated in Fig. 5. It can be observed that the measured broadside AR is maintained below 3 dB from 1253 MHz to 1284 MHz (31 MHz). Good alignment is obtained between measurements and simulations. The measured return loss and broadside AR validate that the proposed antenna can well enclose the BDS B3 band, i.e. 1268.52±10.23 MHz. Fig. 6 shows the simulated and measured broadside CP gain of the proposed antenna. Across the CP bandwidth, the measured CP gain is above 4.0 dBic with a peak gain of 5.1 dBic at 1268 MHz. The differences between simulated and measured results are probably attributed to the fact that the air gap may slightly deviate from the designed value. Furthermore, the inconsistency of the substrate, fabrication tolerance, as well as inductive effect of soldering may also contribute to the observed discrepancies. The simulated radiation efficiency as shown in Fig. 6 is maintained above 90% across the BDS B3 band.

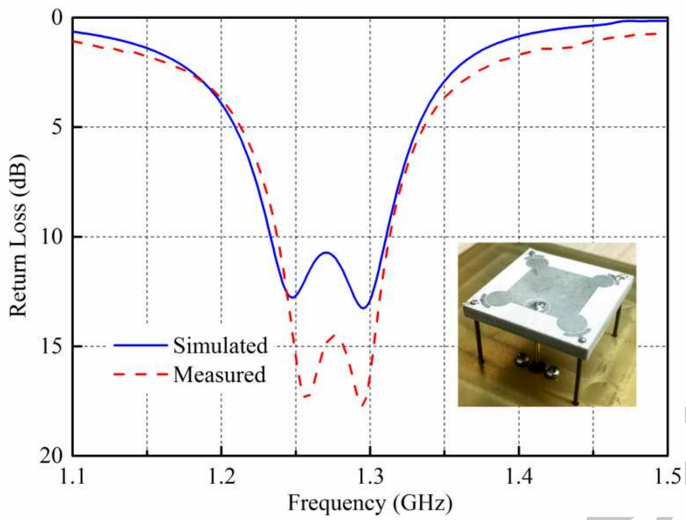

Fig. 4. Simulated and measured return loss of the proposed antenna.

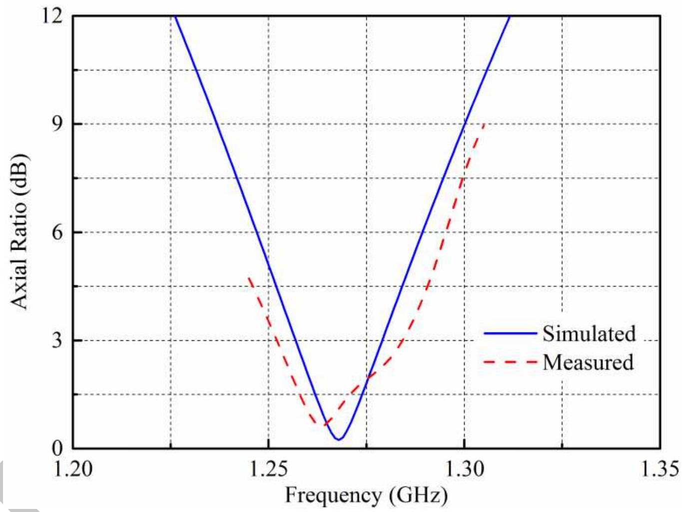

Fig. 5. Simulated and measured broadside AR of the proposed antenna.

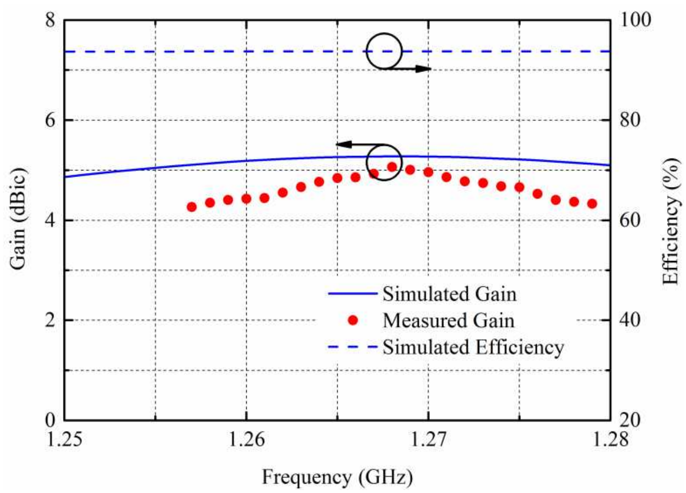

Fig. 6. Simulated and measured broadside gain and efficiency of the proposed antenna.

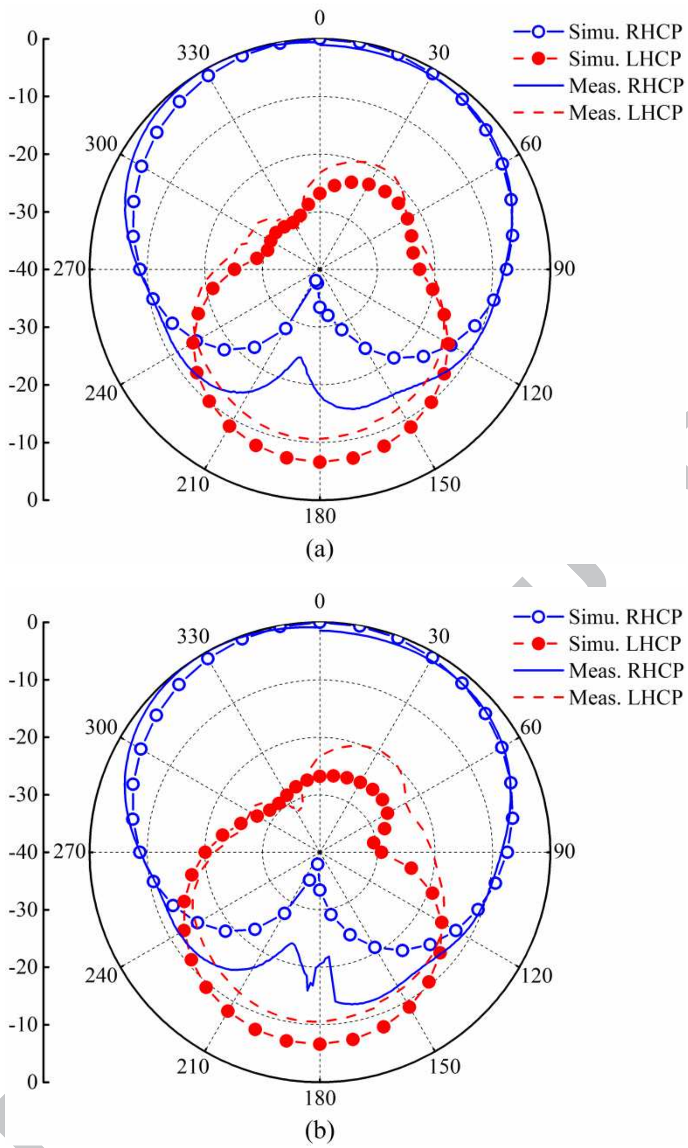

Fig. 7. Simulated and measured radiation patterns at 1268 MHz.

(a) *x-z* plane. (b) *y-z* plane.

The farfield radiation patterns of the prototype antenna have been measured in an anechoic chamber. Fig. 7(a) and (b) present the normalized simulated and measured radiation patterns in *x-z* and *y-z* planes, respectively, at 1268 MHz. Reasonable agreement between simulations and measurements can be seen. The 3-dB AR beamwidth of the antenna is almost wider than 180° in the whole upper hemisphere for both planes, except for a very small angle range just above the horizon in *y-z* plane. Therefore, thanks to its miniaturized aperture size and simple single-feed configuration, the proposed antenna can be potentially deployed for portable BDS receivers and small BDS antenna arrays.

Table 2 summarizes the performance comparison of the proposed antenna and some other reported ones in terms of electrical size, 10-dB return loss bandwidth, 3-dB AR bandwidth, gain and feed configuration. In Table 2, RLBW and ARBW stands for return loss and AR bandwidths, respectively. The proposed antenna exhibits the smallest aperture size and largest gain. Although the antennas reported in [19–22] have much lower profile, the 3-dB ARBWs are narrower than 1.1%, which is inadequate to cover the BDS B3 band. The antenna in [31] owns the largest 3-dB ARBW. However, the dual-feed configuration increases the structural complexity and fabrication cost.

Table 2. Performance comparison of the proposed antenna and other reported ones.

Ant.	Size ($\lambda_0 \times \lambda_0 \times \lambda_0$)	10-dB RLBW (%)	3-dB ARBW (%)	Gain (dBic)	Feed
[19]	0.273 × 0.273 × 0.013	2.0	0.7	3.8	Single
[20]	0.288 × 0.288 × 0.012	2.5	0.5	4.3	Single
[22]	0.240 × 0.240 × 0.019	1.8	1.1	4.2	Single
[30]	0.174 × 0.174 × 0.026	3.3	0.7	3.8	Single
[31]	0.143 × 0.143 × 0.067	12.3	11.9	2.0	Dual
[32]	0.186 × 0.176 × 0.048	4.8	1.5	4.9	Single
Proposed	0.125 × 0.125 × 0.074	5.9	2.4	5.1	Single

4. CONCLUSION

A single-feed miniaturized circularly polarized patch antenna has been proposed and studied in this paper. Rather than the conventional placement strategy of shorting pins, four L-shaped shorting strips are coupled to the patch radiator that not only contribute to the size reduction but also provide capability for broader band operation. Furthermore, the capacitive probe feed permits the circular polarization and impedance matching characteristic of the antenna being tuned independently. An antenna prototype operated at BDS B3 band has been designed and validated. The antenna has obtained compact size ($\lambda_0/8 \times \lambda_0/8 \times \lambda_0/13.6$), adequate impedance and circular polarization bandwidth (75 MHz and 31 MHz, respectively), moderate gain (4.0 dBic), and wide circular polarization beamwidth (170°). Therefore, the proposed antenna can be a good antenna element for small BDS arrays and portable BDS applications.

ACKNOWLEDGEMENT

This work was supported by the China Postdoctoral Science Foundation [grant number 2018M631161]; the Postdoctoral Science Foundation of Shaanxi Province, China [grant number 2017BSHYDZZ14]; the Fundamental Research Funds for the Central Universities [grant number XJTU1191329860]; the Natural Science Foundation of Shaanxi Province, China [grant number 2018JQ6081]; the Technology Program of Shenzhen [grant number JCYJ20170816100722642]; and the Shaanxi Provincial Key Research and Development Plan of China [grant number 2017ZDXM-GY-009].

REFERENCES

[1] Alibakhshi-Kenari M, Limiti E, Naser-Moghadasi M, Virdee BS, Sadeghzadeh RA. A new wideband planar antenna with band-notch functionality at GPS, Bluetooth and WiFi bands for integration in portable wireless systems. Int J Electron Commun 2017;72:79–85.

[2] Alibakhshi-Kenari M, Naser-Moghadasi M, Sadeghzadeh RA, Virdee BS, Limiti E. Traveling-wave antenna based on metamaterial transmission line structure for use in

multiple wireless communication applications. Int J Electron Commun 2016;70(12):1645–50.

[3] Alibakhshi-Kenari M, Naser-Moghadasi M, Sadeghzadeh RA, Virdee BS, Limiti E. Bandwidth extension of planar antennas using embedded slits for reliable multiband RF communications. Int J Electron Commun 2016;70(7):910–9.

[4] Alibakhshi-Kenari M, Virdee BS, Ali A, Limiti E. A novel monofilar-Archimedean metamaterial inspired leaky-wave antenna for scanning application for passive radar systems. Microw Opt Technol Lett 2018;60(8): 2055–60.

[5] Alibakhshi-Kenari M, Virdee BS, Limiti E. Triple-band planar dipole antenna for omnidirectional radiation. Microw Opt Technol Lett 2018;60(4): 1048–51.

[6] Alibakhshi-Kenari M, Virdee BS, See CH, Abd-Alhameed R, Ali A, Falcone F, Limiti E. Wideband printed monopole antenna for application in wireless communication systems. IET Microw Antennas & Propag 2018;12(7):1222–30.

[7] Yu K, Li YS, Liu X. Mutual coupling reduction of a MIMO antenna array using 3-D novel meta-material structures. Appl Comput Electromagn Soc J 2018;33(7):758–63.

[8] Krishna R, Kumar R, Kushwaha N. A circularly polarized slot antenna for high gain applications. Int J Electron Commun 2014;68(11):1119–28.

[9] Fujita K, Yoshitomi K, Yoshida K, Kanaya H. A circularly polarized planar antenna on flexible substrate for ultra-wideband high-band applications. Int J Electron Commun 2015;69(9):1381–6.

[10] Li YS, Mittra R. A three-dimensional circularly polarized antenna with a low profile and a wide 3-dB beamwidth. J Electromagn Waves Appl 2016;30(1):89–97.

[11] Li JX, Shi JW, Li LM, Khan TA, Chen J, Li YS, Zhang AX. Dual-band annular slot antenna loaded by reactive components for dual-sense circular polarization with flexible frequency ratio. IEEE Access 2018, to be published. DOI: 2018. 10.1109/ACCESS.2018.2877425.

[12] Kaplan ED, Hegarty CJ. Understanding GPS: principles and applications. 2nd ed. Norwood: Artech House; 2006.

[13] Fante RL, Vaccaro JJ. Wideband cancellation of interference in a GPS receive array. IEEE Trans Aerosp Electron Syst 2000;36(2):549–64.

[14] Lambert JR, Balanis CA, DeCarlo D. Spherical cap adaptive antennas for GPS. IEEE Trans Antennas Propag 2009;57(2):406–13.

[15] Li JX, Zhang M, Shi HY, Zheng S, Zhang AX. Design and implementation of an adaptive space-time antenna array for GPS receivers. Frequenz 2015;69(3-4):83–7.

[16] Zhou YJ, Chen CC, Volakis JL. Dual band proximity-fed stacked patch antenna for tri-band GPS applications. IEEE Trans Antennas Propag 2007;55(1):220–4.

[17] Zhou YJ, Chen CC, Volakis JL. Single-fed circularly polarized antenna element with reduced coupling for GPS arrays. IEEE Trans Antennas Propag 2008;56(5):1469–72.

[18] Li JX, He B, Fang J, Zhang AX. Compact dual-band proximity-fed circularly polarized patch antenna for BDS applications. Frequenz 2015:69(9-10):407–412.

[19] Nasimuddin, Chen ZN, Qing XM. A compact circularly polarized cross-shaped slotted microstrip antenna. IEEE Trans Antennas Propag 2012;60(3):1584–8.

[20] Nasimuddin, Qing XM, Chen ZN. Compact asymmetric-slit microstrip antennas for circular polarization. IEEE Trans Antennas Propag 2011;59(1):285–8.

[21] Agarwal K, Nasimuddin, Alphones A. RIS-based compact circularly polarized microstrip antennas. IEEE Trans Antennas Propag 2013;61(2):547–54.

[22] Xu HX, Wang GM, Liang JG, Qi MQ, Gao X. Compact circularly polarized antennas combining meta-surfaces and strong space-filling meta-resonators. IEEE Trans Antennas Propag 2013;61(7):3442–50.

[23] Alibakhshi-Kenari M, Virdee BS, Ali A, Limiti E. Extended aperture miniature antenna based on CRLH metamaterials for wireless communication systems operating over UHF to C-band. Radio Sci 2018;53(2):154–65.

[24] Alibakhshi-Kenari M, Virdee BS, Ali A, Limiti E. Miniaturized planar-patch antenna based on metamaterial L-shaped unit-cells for broadband portable microwave devices and multiband wireless communication systems. IET Microw Antennas & Propag 2018;12(7):1080–6.

[25] Alibakhshi-Kenari M, Naser-Moghadasi M, Sadeghzadeh RA, Virdee BS, Limiti E. New compact antenna based on simplified CRLH-TL for UWB wireless communication systems. Int J RF Microw Comput Aided Eng 2016;26(3):217–25.

[26] Alibakhshi-Kenari M, Naser-Moghadasi M, Sadeghzadeh RA, Virdee BS. Metamaterial-based antennas for integration in UWB transceivers and portable microwave handsets. Int J RF Microw Comput Aided Eng 2016;26(1):88–96.

[27] Gupta S, Mumcu G. Dual-band miniature coupled double loop GPS antenna loaded with lumped capacitors and inductive pins. IEEE Trans Antennas Propag 2013;61(6):2904–10.

[28] Waterhouse R. Small microstrip patch antenna. Electron Lett 1995;31(8):604–5.

[29] Yang M, Chen ZN, Lau PY, Qing XM, Yin XX. Miniaturized patch antenna with

grounded strips. IEEE Trans Antennas Propag 2015;63(2):843–8.

[30] Wong H, So KK, Ng KB, Luk KM, Chan CH, Xue Q. Virtually shorted patch antenna for circular polarization. IEEE Antennas Wirel Propag Lett 2010;9:1213–6.

[31] Sun C, Zheng HL, Zhang LF, Liu Y. Analysis and design of a novel coupled shorting strip for compact patch antenna with bandwidth enhancement. IEEE Antennas Wirel Propag Lett 2014;13:1477–81.

[32] Li JX, Guo JY, Zhang AX, Joines WT, Liu QH. Miniaturized single-feed cross-aperture coupled circularly polarized microstrip patch antenna. Progress In Electromagn Res C 2016;63:183–91.

[33] Nasimuddin, Anjani YS, Alphones A. A wide-beam circularly polarized asymmetric-microstrip antenna. IEEE Trans Antennas Propag 2015;63(8):3764–8.

[34] Sievenpiper DF, Dawson DC, Jacob MM, Kanar T, Kim S, Long J, Quarfoth RG. Experimental validation of performance limits and design guidelines for small antennas. IEEE Trans Antenans Propag 2012;60(1):8–19.

[35] Li JX, Shi HY, Li H, Zhang AX. Quad-band probe-fed stacked annular patch antenna for GNSS applications. IEEE Antennas Wirel Propag Lett 2014;13:372–375.